



## Electronic Delivery Cover Sheet

### **WARNING CONCERNING COPYRIGHT RESTRICTIONS**

The copyright law of the United States (Title 17, United States Code) governs the making of photocopies or other reproductions of copyrighted materials. Under certain conditions specified in the law, libraries and archives are authorized to furnish a photocopy or other reproduction. One of these specified conditions is that the photocopy or reproduction is not to be "used for any purpose other than private study, scholarship, or research". If a user makes a request for, or later uses, a photocopy or reproduction for purposes in excess of "fair use", that user may be liable for copyright infringement. This institution reserves the right to refuse to accept a copying order if, in its judgement, fulfillment of the order would involve violation of copyright law.

# Phonon density of states in vanadium

V.F. Sears, E.C. Svensson, and B.M. Powell

**Abstract:** The normalized phonon density of states  $g(\nu)$  of vanadium is accurately determined at room temperature (294 K) from the analysis of neutron inelastic-scattering data obtained using a triple-axis crystal spectrometer with a constant momentum transfer  $Q = 6.5 \text{ \AA}^{-1}$ , ( $1 \text{ \AA} = 10^{-10} \text{ m}$ ) a constant scattered-neutron energy of 8.0 THz, and a variable incident-neutron energy. The energy transfer in the experiment varies from  $-1.9$  to 10.0 THz, and the energy resolution (FWHM) is 0.35 THz at the elastic position. Necessary corrections are made for background scattering, multiple scattering, multiphonon scattering, absorption and self-shielding, and for the spatial inhomogeneity of the incident beam. The resulting  $g(\nu)$  distribution has an average statistical precision of about 3% and is characterized by peaks at 4.9 and 6.9 THz, which we attribute to transverse and longitudinal phonons, respectively, and by a cutoff at about 8.1 THz. The peaks in our  $g(\nu)$  distribution are much more clearly resolved than in any previous work on vanadium. We also see a small shoulder in  $g(\nu)$  in the region 2–3 THz, but it is far less pronounced than in some of the earlier experiments on vanadium. Below 2 THz we find that  $g(\nu) = a\nu^2$ , and the observed value of  $a$  leads to a Debye temperature that is in excellent agreement with that obtained from the measured elastic constants of vanadium at room temperature. A theoretical  $g(\nu)$  distribution calculated by Clark on the basis of a nearest- and next-nearest-neighbor central force model is in generally good agreement with our results although it differs in some details. In particular, Clark's theory predicts that the transverse peak should be slightly more intense than the longitudinal peak, whereas our experimental results indicate the opposite.

**Résumé :** La densité normalisée  $g(\nu)$  des états de phonons du vanadium est calculée avec précision à température ambiante (294 K), à partir de l'analyse des données de diffusion élastique des neutrons obtenues en utilisant un spectromètre à axe triple avec un transfert d'impulsion constant  $Q = 6,5 \text{ \AA}^{-1}$  ( $1 \text{ \AA} = 10^{-10} \text{ m}$ ), une valeur constante 8,0 THz de l'énergie des neutrons diffusés et une énergie variable des neutrons incidents. Dans l'expérience, le transfert d'énergie varie de  $-1,9$  à 10,0 THz, et la résolution en énergie (FWHM) est 0,36 THz à la position élastique. Les corrections nécessaires sont effectuées pour la diffusion de fond, la diffusion multiple, la diffusion multiphonon, l'absorption et l'effet auto-écran, ainsi que pour l'hétérogénéité du faisceau incident. La distribution  $g(\nu)$  résultante a une précision statistique moyenne d'environ 3% et est caractérisée par des pics, à 4,9 et 6,9 THz, que nous attribuons à des phonons transversaux et longitudinaux, respectivement, et par une coupure à environ 8,1 THz. Les pics dans notre distribution  $g(\nu)$  sont beaucoup plus clairement résolus que dans tous les travaux précédents sur le vanadium. On voit aussi, dans la région 2 à 3 THz de la courbe de  $g(\nu)$ , un petit épaulement qui est cependant beaucoup moins prononcé que dans certaines expériences antérieures sur le vanadium. Au-dessous de 2 THz nous trouvons que  $g(\nu) = a\nu^2$ . La valeur observée pour  $a$  donne une température de Debye qui est en excellent accord avec celle qu'on obtient à partir des valeurs mesurées des constantes élastiques du vanadium à température ambiante. Une distribution  $g(\nu)$  théorique calculée par Clark sur la base d'un modèle de forces centrales entre premier et second voisins est généralement en bon accord avec nos résultats tout en étant différente pour certains détails. En particulier, la théorie de Clark prédit que le pic transversal devrait être légèrement plus intense que le pic longitudinal, alors que nos résultats expérimentaux indiquent le contraire.

[Traduit par la rédaction]

## 1. Introduction

It was originally shown by Placzek and Van Hove [1] in 1954 that the phonon density of states  $g(\nu)$  of a crystal could, in principle, be determined directly by means of incoherent in-

elastic neutron scattering. The first such experiment was carried out on vanadium the following year by Brockhouse [2] using an early version of the triple-axis crystal spectrometer, and was one of the many pioneering experiments for which

Received June 19, 1995. Accepted August 31, 1995.

V.F. Sears,<sup>1</sup> E.C. Svensson, and B.M. Powell, Atomic Energy of Canada Limited, Chalk River Laboratories, Chalk River, On K0J 1J0, Canada.

<sup>1</sup> Author to whom all correspondence should be addressed either at the above address or **Telephone:** (613) 584 8811 extension 4071. **FAX:** (613) 584 1849. **e-mail:** searsv@crl.aecl.ca

Professor Brockhouse was recently awarded the Nobel Prize in physics.

Vanadium is the ideal material for this kind of experiment because

(i) it is an almost totally (99.6%) incoherent scatterer and  
 (ii) the atoms occupy the sites of a cubic Bravais lattice (the bcc structure) so that, to the extent that multiphonon scattering is negligible, the observed inelastic scattering is directly proportional to the phonon density of states [1].

In all other incoherently scattering materials, the effective density of states obtained from such experiments is weighted by the phonon polarization vectors. In practice, however, vanadium does not provide an easy experiment because, if one wishes to measure  $g(\nu)$  with high resolution, it is necessary to use a relatively small momentum transfer  $Q$  for which the inelastic scattering is very weak, and extremely long counting times are then required to achieve high statistical precision.

Nevertheless, many neutron-scattering experiments [3–14] were performed on vanadium in the period 1956–1967 to determine the phonon density of states, but apparently only one [15] in more recent years. With the exception of the present work, which was done using a modern triple-axis crystal spectrometer, all these other experiments were performed using time-of-flight spectrometers, mostly with a beryllium-filtered incident beam. Although most of these experiments yielded roughly similar  $g(\nu)$  results, with reasonably well-resolved transverse and longitudinal peaks, they differed considerably in their detailed shapes owing to differences in energy resolution and statistical precision, and in the way the authors corrected for effects such as multiphonon scattering and multiple scattering.

In the past 5 years, we have collaborated with a number of groups in many neutron inelastic-scattering experiments at the NRU reactor at Chalk River to determine the phonon density of states in various hydrogenous materials [16–23]. The initial motivation for the present experiment on vanadium was simply to obtain a benchmark for this work, and to test the method used for making multiphonon corrections. However, it soon became apparent that, if we were going to repeat this classic experiment, we should try to determine  $g(\nu)$  with much higher resolution and statistical precision than had been achieved in any of the earlier experiments mentioned above in order to resolve some of the discrepancies that exist in that work and to provide a more accurate test of available theoretical calculations [24]. We have also been able to shed some light on a long-standing discrepancy between the Debye temperatures of vanadium determined from specific heat and from elastic-constant measurements [25].

## 2. Experiment

The experiment was performed using the N5 triple-axis crystal spectrometer at NRU with a Si (331) monochromator and a Ge (113) analyzer. The scattered-neutron distributions were obtained by varying the incident-neutron energy with a constant momentum transfer  $Q = 6.5 \text{ \AA}^{-1}$  and a constant scattered-neutron energy of 8.0 THz. The resulting energy transfer  $\nu$  varied from  $-1.9$  to 10.0 THz in steps of 0.1 THz and, in the region of the transverse and longitudinal peaks (4.1 to 8.3 THz), additional scans were taken with a smaller step size of 0.05 THz. The energy resolution (FWHM) was

0.35 THz at the elastic position. It was necessary to accumulate data over a total period of about two months to obtain sufficient intensity in the inelastic region (typically 700 to 1300 counts) to enable us to determine  $g(\nu)$  with an average statistical precision of 3%. The corresponding background, as determined from measurements in the absence of the sample, was about 150 counts.

The nominally pure vanadium sample was in the form of a plane slab 0.457 cm thick, and was masked to give an effective height of 8.84 cm and an effective width of 5.04 cm. For a neutron beam of energy 8.0 THz that is normally incident on the sample, we estimate that 14% of the incident neutrons are scattered, 12% are absorbed, and the remaining 74% are transmitted. For the scattered neutrons, 83% are scattered once, 15% are scattered twice, and 2% are scattered three or more times. The experiment was performed in symmetric transmission geometry with the sample at room temperature (about 294 K).

## 3. Analysis

At each point in the experimental scans, we recorded the total number of detector counts that were obtained in the time required to accumulate a prescribed number of monitor counts. The total number of such detector counts can be expressed as

$$C_t = C_s + C_b \quad (3.1)$$

where  $C_s$  is the contribution from scattering by the sample and  $C_b$  is the background observed in the absence of the sample. Figure 1 shows the values of  $C_t$  (dots) and  $C_b$  (crosses) obtained in the present experiment. (The data in this figure have been compounded from a large number of scans that were taken with various monitor settings, and are normalized to  $4.2 \times 10^7$  monitor counts.) The corresponding values of  $C_s$  are shown by the dots in Fig. 2.

The net scattering by the sample is the sum of two terms

$$C_s = C_{ss} + C_{ms} \quad (3.2)$$

where  $C_{ss}$  is the contribution from single scattering and  $C_{ms}$  that from multiple scattering. The former can be expressed as

$$C_{ss} = NABS(Q, \nu) \quad (3.3)$$

where  $N$  is the normalization factor,  $A$  is the correction for absorption and self-shielding, and  $B$  is the correction for the lateral inhomogeneity in the incident beam, which we shall call the beam profile correction. Finally,  $S(Q, \nu)$  is the Van Hove incoherent scattering function in which  $\hbar Q$  and  $h\nu$  are the momentum and energy transferred from a neutron to the sample in a collision. Strictly speaking, in expression (3.3) the function  $S(Q, \nu)$  should be folded with the instrumental resolution function. However, we need not show this explicitly.

Since the experiment was performed with a fixed scattered-neutron energy and variable incident energy, the normalization factor  $N$  in (3.3) is constant across the scan. The correction factor  $A$  was calculated as described in ref. 26, and  $B$  was determined experimentally by measuring the scattering from a thin polyethylene rod that was scanned across the

**Fig. 1.** Total counts  $C_t$  (dots) and background counts  $C_b$  (crosses) observed in a vanadium sample at  $T = 294$  K with a momentum transfer  $Q = 6.5 \text{ \AA}^{-1}$ . At the elastic position  $C_t = 52.990$ .

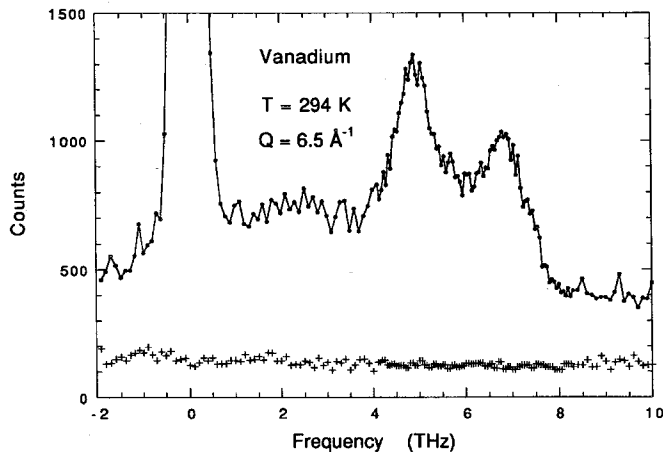


**Fig. 2.** Net counts  $C_s$  (dots). The broken line is the estimated multiphonon scattering, calculated as described in Appendix.

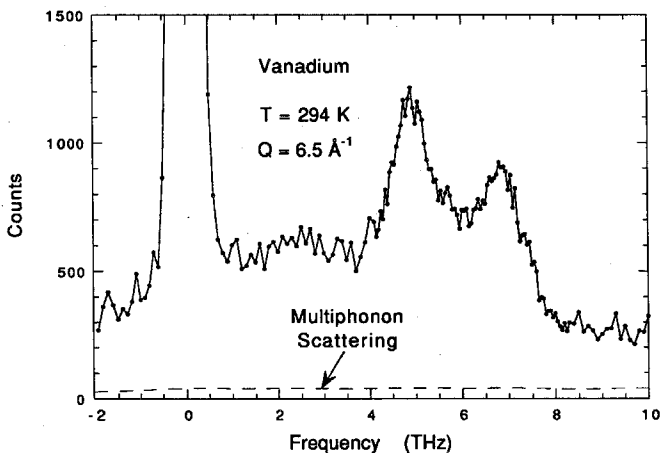
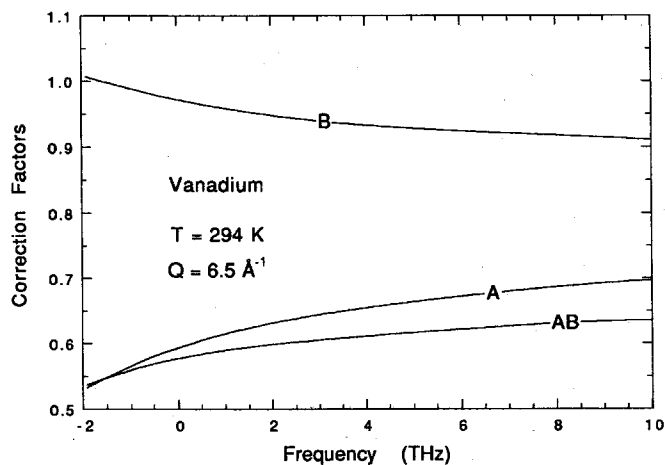


**Fig. 3.** Calculated correction factor for absorption and self-shielding  $A$ , measured correction factor for the inhomogeneity of the incident beam  $B$ , and the product  $AB$ .



beam at the position of the sample for a series of incident-neutron energies. The correction factors  $A$  and  $B$  are shown as a function of  $\nu$  in Fig. 3 together with the product  $AB$ . It will be noted that the decrease in  $B$  with increasing  $\nu$  is partly compensated by the increase in  $A$ , so that the product  $AB$  increases by only 9% in the region 0–8 THz.

The multiphonon expansion of the incoherent scattering function is discussed in Appendix A, and can be expressed in the form

$$S(Q, \nu) = e^{-2W} \left[ \delta(\nu) + \left( \frac{\nu_r}{\nu} \right) \frac{g(\nu)}{1 - \exp(-\nu/\nu_0)} + \dots \right] \quad (3.4)$$

in which the first term represents the elastic scattering, the second term the one-phonon scattering, and the dots the multiphonon scattering. Here,  $e^{-2W}$  is the Debye-Waller factor, in which  $2W = (Qu)^2$  and  $u$  is the root-mean-square (rms) displacement of an atom in the direction of  $Q$ . Also,  $h\nu_r$  is the recoil energy, which is defined by the relation  $h\nu_r = (\hbar Q)^2/2M$  in which  $M$  is the atomic mass, and  $h\nu_0 = k_B T$ , where  $T$  is the temperature. In particular,  $\nu_0 = 6.13$  THz in our experiments, where  $T = 294$  K. Finally,  $g(\nu)$  is the phonon density of states, which is taken to be an even function of  $\nu$  and is normalized such that

$$\int_0^\infty g(\nu) d\nu = 1 \quad (3.5)$$

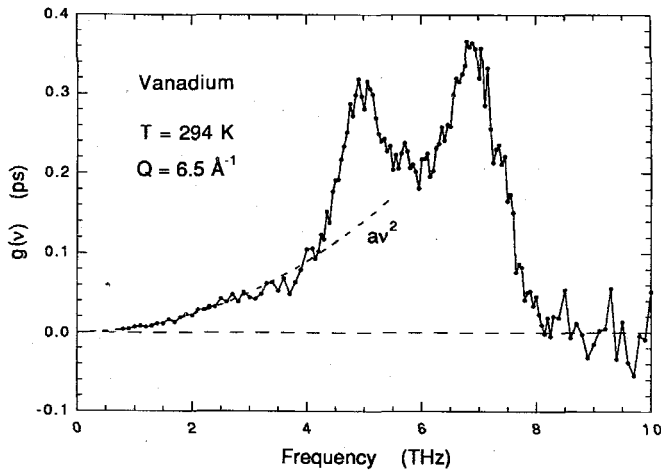
The multiphonon contribution to  $C_{ss}$  was calculated self-consistently from our experimentally determined  $g(\nu)$  distribution, as described in Appendix A, and is shown by the broken line in Fig. 2. This contribution varies by only 10% over the frequency range 0–8 THz. It is reasonable to assume that the multiple inelastic-scattering contribution to  $C_{ms}$  in (3.2) is also approximately constant in this region. For example, the double one-phonon scattering and the two-phonon single scattering are determined by similar integrals and, hence, can be expected to have roughly similar shapes. (A more detailed discussion of the multiphonon and multiple scattering is given in Appendices A and B.) The observed scattering between 8.5 and 10.0 THz, which has an average value of 270 counts, represents the sum of the multiphonon single scattering and the multiple inelastic scattering, and this average value was then used to separate the one-phonon scattering from the observed net scattering  $C_s$  in Fig. 2 and, hence, to obtain the phonon density of states  $g(\nu)$  with the help of (3.4). The resolution-broadened elastic peak was fitted to a Gaussian function to separate it from the inelastic scattering, and the full width at half maximum (FWHM) of the elastic peak was found to be 0.353(3) THz. This enabled us to obtain meaningful values of  $g(\nu)$  for frequencies down to about 0.8 THz.

Figure 4 shows the phonon density of states  $g(\nu)$  that has been determined in this way. The distribution was put on an absolute scale with the help of the normalization condition (3.5), and is characterized by peaks at about 4.9 and 6.9 THz, which we attribute to transverse and longitudinal phonons, respectively, and by a cutoff at about 8.1 THz.

In a three-dimensional crystal, the phonon density of states has the characteristic property [27]

$$g(\nu) \rightarrow a\nu^2 \quad \text{as} \quad \nu \rightarrow 0 \quad (3.6)$$

**Fig. 4.** The phonon density of states  $g(\nu)$  for room-temperature vanadium determined in the present work from neutron inelastic scattering measurements at  $Q = 6.5 \text{ \AA}^{-1}$ . The broken-line curve is the inferred low-frequency limit of this function.



**Fig. 5.** The quantity  $g(\nu)/\nu^2$  for room-temperature vanadium determined in the present work from neutron inelastic scattering measurements at  $Q = 6.5 \text{ \AA}^{-1}$ .

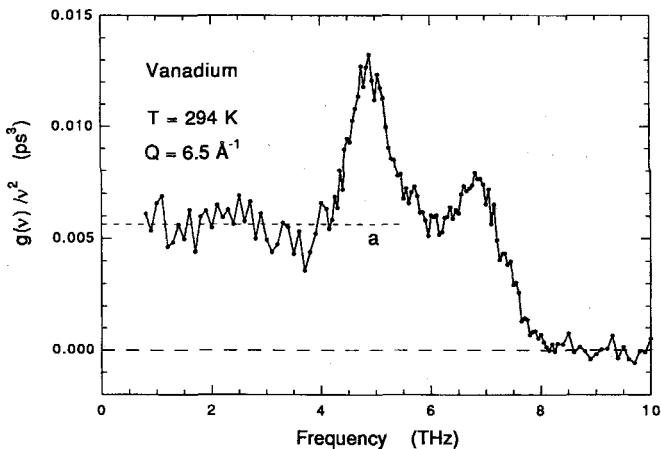


Figure 5 shows that, apart from fluctuations due to counting statistics, the quantity  $g(\nu)/\nu^2$  determined in the present work is, indeed, constant at low frequency. Taking the average of the 13 points in the range  $0.8 \leq \nu \leq 2.0 \text{ THz}$ , we find that  $a = 0.00564(21) \text{ ps}^3$ . This asymptotic limit is indicated by the short broken lines in Figs. 4 and 5.

## 4. Discussion

### 4.1. Phonon density of states

During the past 40 years, many neutron-scattering experiments [2–15] have been performed on vanadium to determine the phonon density of states, and the results are summarized in Table 1 where we list the various values that have been obtained for the frequencies of the transverse peak ( $\nu_T$ ), the longitudinal peak ( $\nu_L$ ), and the cutoff ( $\nu_{\max}$ ). The cutoff is not determined very precisely in most of these experiments,

**Table 1.** Frequencies of the transverse peak ( $\nu_T$ ), the longitudinal peak ( $\nu_L$ ), and the cutoff ( $\nu_{\max}$ ) in the phonon density of states  $g(\nu)$  of room-temperature vanadium determined from various neutron inelastic-scattering experiments.

$\nu_T$ (THz)	$\nu_L$ (THz)	$\nu_{\max}$ (THz)	Authors (Year)	Ref.
		7.3	Brockhouse (1955)	2
	6.4	10.6	Carter et al. (1956)	3
4.8	6.5	8.5	Stewart and Brockhouse (1958)	4
5.0	6.9	9.0	Eisenhauer et al. (1958)	5
4.8	6.5	9.0	Turberfield and Egelstaff (1962)	7
5.2	6.9	10.1	Chernoplekov et al. (1963)	8
4.8	6.5	9.0	Haas et al. (1963)	10
4.9	6.5	8.7	Mozer et al. (1965)	12
5.2	6.6	8.8	Gläser et al. (1965)	13
4.8	6.9	8.0	Page (1967)	14
5.3	7.4	8.6	Kamal et al. (1978)	15
4.9	6.9	8.1	Present work	

and the values that we have assigned for  $\nu_{\max}$  in Table 1 are simply intended as rough estimates. With the exception of the original Brockhouse experiment [2] and the present work, both of which were done with triple-axis crystal spectrometers, all the other experiments were performed using time-of-flight spectrometers, mostly with a beryllium-filtered incident beam. All previous work was done with lower resolution and (or) lower statistical precision than in the present study. In particular, the peaks in our  $g(\nu)$  distribution are much more clearly resolved than in any of the previous work mentioned above. Nevertheless, our resolution and statistical precision are still not adequate to resolve the Van Hove singularities in  $g(\nu)$ , which arise from the existence of saddle points on the phonon dispersion surface [28]. The instrumental resolution will, of course, affect the positions of the peaks, and this probably accounts for most of the discrepancies in Table 1.

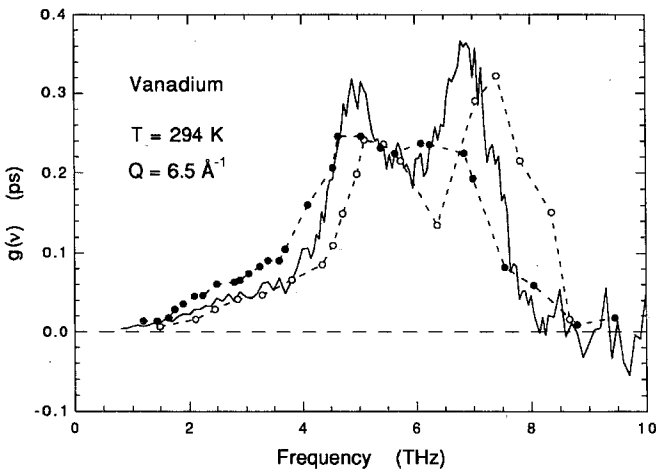
In most of the previous work on vanadium [4, 5, 7–14], there is a small shoulder in  $g(\nu)$ , or a corresponding small peak in  $g(\nu)/\nu^2$ , in the region 2–3 THz that has sometimes been interpreted in terms of the Kohn effect [11, 13]. Although such a feature is also discernible in our results (see Figs. 4 and 5), it is far less pronounced than in some of the earlier experiments [7, 11, 14].

Figure 6 shows a comparison of our results (continuous line) with the early results of Stewart and Brockhouse [4] (filled circles), and with the most recent work of Kamal et al. [15] (open circles). The  $g(\nu)$  distribution obtained by Stewart and Brockhouse is largely consistent with ours when one allows for the difference in resolution, but the two peaks in the results of Kamal et al. occur at higher frequencies than in either our results or those of any earlier authors (see Table 1).

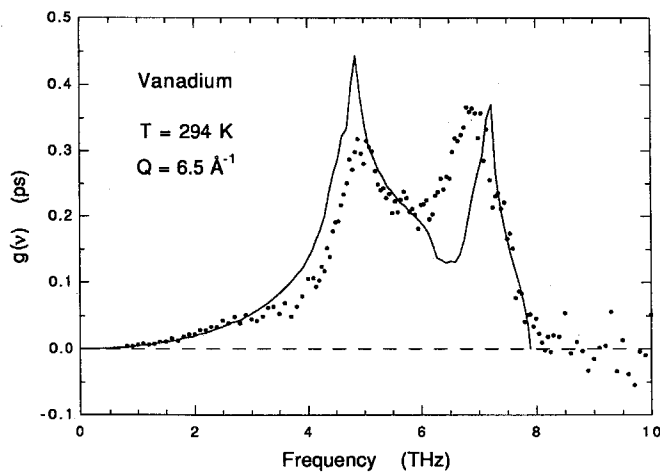
### 4.2. Clark's model

Many years ago Clark [24] carried out a general investigation of the phonon density of states in a body-centered cubic (bcc) structure on the basis of the Born – von Kármán theory of lattice vibrations. For a model with nearest- and next-nearest-neighbor central forces, he showed that the shape of  $g(\nu)$  is

**Fig. 6.** Phonon density of states  $g(\nu)$  for room-temperature vanadium determined by various neutron inelastic scattering measurements. The continuous line shows our present results, the filled circles are those of Stewart and Brockhouse [4], and the open circles are those of Kamal et al. [15].



**Fig. 7.** Comparison of the phonon density of states  $g(\nu)$  for room-temperature vanadium determined in the present experiment (dots) with the theoretical distribution calculated by Clark [24] and scaled as described in the text (continuous line).



uniquely determined by a single parameter, the ratio of the two force constants  $\alpha_1$  and  $\alpha_2$ , and that this parameter is itself determined by the elastic constants, i.e.,

$$\beta \equiv \frac{\alpha_2}{\alpha_1} = \frac{c_{11} - c_{12}}{3c_{44}} \quad (4.1)$$

He then calculated  $g(\nu)$  for 100 equally spaced frequency intervals in the range  $0 \leq \nu \leq \nu_{\max}$  and for 18 representative values of the ratio  $\beta$ , including the value  $\beta = 0.82$  that he obtained from the measured elastic constants of vanadium at 4.2 K [25]. However, the individual values of  $\alpha_1$  and  $\alpha_2$  for vanadium were unknown so that he was unable to determine  $\nu_{\max}$  itself.

Figure 7 shows a comparison of the phonon density of states  $g(\nu)$  for room-temperature vanadium determined in the present experiment (dots) with the theoretical distribu-

**Table 2.** Comparison of the mean-square displacements  $u^2$  calculated at various temperatures  $T$  using the phonon density of states  $g(\nu)$  determined by Kamal et al. [15] and the present work. The last column lists the values of  $u^2$  at two temperatures that were obtained from measured X-ray Debye–Waller factors [29].

$T(K)$	$u^2(\text{\AA}^2)$		
	Ref. 15	Present work	Ref. 29
4.2	0.0020	0.001 95	0.001 93(8)
10.0	0.0020	0.001 95	
20.0	0.0020	0.001 98	
40.0	0.0021	0.002 07	
100.0	0.0028	0.002 74	
150.0	0.0036	0.003 55	
296.0	0.0062	0.006 29	0.006 56(13)

tion calculated by Clark for  $\beta = 0.82$  (continuous line). In plotting Clark's results, we put  $\nu_{\max} = 7.9$  THz, which is the value that best fits our experimental phonon density of states at large  $\nu$ , and relation (3.5) was used to obtain an absolute normalization of the distribution. We then find that in Clark's distribution  $\nu_T = 4.85$  THz and  $\nu_L = 7.19$  THz, which are close to the values 4.9 and 6.9 THz that we obtained from our neutron measurements (see Table 1). The theoretical  $g(\nu)/\nu^2$  curve for  $\nu \leq 2.0$  THz has an essentially constant value given by  $a = 0.0049$  ps<sup>3</sup>, which is slightly less than our experimentally determined value of  $0.0056(2)$  ps<sup>3</sup>.

Apart from the effects of instrumental resolution, Clark's theoretical distribution in Fig. 7 is in general qualitative agreement with our experimental  $g(\nu)$  results. The main discrepancy lies in the fact that the theory predicts that the transverse peak should be slightly more intense than the longitudinal peak, whereas our results indicate the opposite. Clark's model is certainly oversimplified in its assumption of only nearest- and next-nearest-neighbor central forces. In the Born – von Kármán analysis of the measured phonon dispersion curves for similar bcc metals (e.g., niobium and tantalum), it is necessary to include the seventh to tenth nearest-neighbor interactions to obtain detailed quantitative agreement with experiment. Thus, the fact that Clark's  $g(\nu)$  results are in only qualitative agreement with our experimental distribution is not too surprising.

### 4.3. Debye–Waller factor

Having determined the phonon density of states  $g(\nu)$ , we can now calculate the Debye–Waller factor as described in Appendix A. Thus, we find from (A7) that at  $T = 294$  K the quantity  $\gamma_0 = 0.628$  ps, and from (A13) that at  $Q = 6.5$  Å<sup>-1</sup> the recoil energy is  $\nu_r = 0.419$  THz. Hence, from (A12), we get  $2W = 0.263$  and  $e^{-2W} = 0.769$ . The corresponding rms displacement of an atom is then found to be  $u = 0.0789$  Å.

In a first approximation,  $g(\nu)$  can be assumed to be independent of temperature so that the variation of  $u$  and  $2W$  with  $T$  is simply due to the change in the Bose–Einstein population of the phonons in the crystal. Table 2 shows a comparison of the mean-square displacements  $u^2$  calculated by Kamal et al. [15] at various temperatures with the corresponding values that we have calculated from our results. The good agreement between the two sets of values is remarkable when one con-

**Table 3.** Values of the Debye temperature  $\Theta_D$  that characterizes the  $v^2$  behavior of the phonon density of states  $g(v)$  at small  $v$  as determined by various methods for vanadium at two temperatures  $T$ .

Method	$\Theta_D$ (K)		Authors (Year)	Ref.
	$T = 4.2$ K	$T = 294$ K		
Specific heat	273		Worley et al. (1955)	30
	338(5)		Corak et al. (1956)	31
	315		Cheng et al. (1962)	32
Elastic constants	399.3	388	Alers (1960)	25
Neutron scattering		389(5)	Present work	

siders the rather large discrepancies in the underlying  $g(v)$  distributions shown in Fig. 6. This would seem to indicate that the value of  $u$  is not very sensitive to the detailed shape of the phonon density-of-states curve. The right-hand column in Table 2 lists the values of  $u^2$  at two temperatures that were obtained directly from the Debye–Waller factors determined from X-ray diffraction measurements on a powder sample of vanadium [29]. The agreement is very good at 4.2 K but the X-ray value is 6% larger than our value at room temperature.

#### 4.4. Debye temperature

Vanadium is a superconductor with a transition temperature  $T_s = 5.03$  K. At temperatures just above  $T_s$  the observed specific heat [30–32] has the usual form for a normal metal,

$$C_V = \gamma T + \frac{12\pi^4 R}{5} \left( \frac{T}{\Theta_D} \right)^3 \quad (4.2)$$

in which the first term is the contribution from the free electrons and the second term that from the lattice vibrations. The  $T^3$  behavior of the lattice specific heat is a direct consequence of the asymptotic relation (3.6) and the fact that only the low-frequency modes of vibration are thermally populated at low temperatures.

The Debye temperature  $\Theta_D$  is determined from the proportionality constant  $a$  in (3.6) by means of the relations  $a = 3v_D^{-3}$  and  $hv_D = k_B\Theta_D$ , in which  $v_D$  is the Debye frequency. Using the value  $a = 0.00564(21)$  ps<sup>3</sup>, which we obtained in Sect. 3 from the analysis of our present neutron data, we find that  $v_D = 8.10(10)$  THz and, hence, that  $\Theta_D = 389(5)$  K. The fact that this value of  $v_D$  is the same as we found for the cutoff frequency  $v_{\max}$  (see Table 1) is clearly accidental since the  $T^3$  behavior of the lattice specific heat at low temperatures does not require that  $g(v) = av^2$  for all  $v \leq v_{\max}$ . In other words, it is not based on the Debye model.

Table 3 shows a comparison of the values of  $\Theta_D$  for vanadium that have been determined by three different methods at two temperatures  $T$ . The value  $\Theta_D = 388$  K obtained by Alers [25] from the measured elastic constants of room-temperature vanadium is in excellent agreement with our value,  $389 \pm 5$  K, but both are considerably larger than the values obtained from low-temperature specific-heat measurements [30–32]. This large discrepancy is very surprising since, for all other cubic metals that have been examined [33], the values of  $\Theta_D$  obtained from specific-heat measurements are in good

agreement with those obtained from elastic-constant measurements. Alers also measured the elastic constants of vanadium at the temperature of liquid helium, where the specific-heat measurements were performed, and found a small increase in the value of  $\Theta_D$ , which makes the discrepancy with the specific-heat results even larger (see Table 3). Such an increase in  $\Theta_D$  is expected from anharmonic effects that lead to thermal expansion and an accompanying softening of the lattice vibrations at the higher temperature.

## 5. Summary and conclusions

The normalized phonon density of states  $g(v)$  of vanadium has been accurately determined at room temperature from the analysis of neutron inelastic-scattering data obtained using a triple-axis crystal spectrometer with a constant momentum transfer  $Q = 6.5 \text{ \AA}^{-1}$  and a constant scattered-neutron energy of 8.0 THz. The energy transfer in the experiments was varied from  $-1.9$  to 10.0 THz, and the energy resolution (FWHM) was 0.35 THz at the elastic position. Necessary corrections were made for background scattering, multiple scattering, multiphonon scattering, absorption and self-shielding, and for the spatial inhomogeneity of the incident beam.

The resulting  $g(v)$  distribution has an average statistical precision of about 3% and is characterized by peaks at 4.9 and 6.9 THz, which we attribute to transverse and longitudinal phonons, respectively, and by a cutoff at about 8.1 THz. The peaks in our  $g(v)$  distribution are much more clearly resolved than in any previous work on vanadium [2–15]. We also see a small shoulder in  $g(v)$  in the region 2 to 3 THz, but it is far less pronounced than in some of the earlier experiments on vanadium. Below 2 THz we find that  $g(v) = av^2$ , and the observed value of  $a$  leads to a Debye temperature that is in good agreement with that obtained from the measured elastic constants of vanadium at room temperature [25]. The mean-square displacements  $u^2$ , calculated at various temperatures from our  $g(v)$  distribution, agree well with similar calculations by Kamal et al. from their neutron results [15]. Our calculated values of  $u^2$  also agree with those from available X-ray Debye–Waller factor measurements [29].

The theoretical  $g(v)$  distribution calculated by Clark [24] on the basis of a nearest- and next-nearest-neighbor central force model is in general qualitative agreement with our results although it differs in some details. In particular, Clark's theory predicts that the transverse peak should be slightly more intense than the longitudinal peak, whereas our experimental results indicate the opposite.

## Acknowledgement

The valuable technical assistance of M.M. Potter and D.C. Tennant is gratefully acknowledged.

## References

1. G. Placzek and L. Van Hove. *Phys. Rev.* **93**, 1207 (1954).
2. B.N. Brockhouse. *Can. J. Phys.* **33**, 889 (1955).
3. R.S. Carter, D.J. Hughes, and H. Palevsky. *Phys. Rev.* **104**, 271 (1956).
4. A.T. Stewart and B.N. Brockhouse. *Rev. Mod. Phys.* **30**, 250 (1958).
5. C.M. Eisenhauer, I. Pelah, D.J. Hughes, and H. Palevsky. *Phys. Rev.* **109**, 1046 (1958).
6. K.C. Turberfield and P.A. Egelstaff. *In Inelastic scattering of neutrons in solids and liquids*. IAEA, Vienna. 1961. p. 581.
7. K.C. Turberfield and P.A. Egelstaff. *Phys. Rev.* **127**, 1017 (1962).
8. N.A. Chernoplekov, M.G. Zemlyanov, and A.G. Chicherin. *Sov. Phys. JETP*, **16**, 1472 (1963).
9. M.G. Zemlyanov, Y.M. Kagan, N.A. Chernoplekov, and A.G. Chicherin. *In Inelastic scattering of neutrons in solids and liquids*. Vol. II. IAEA, Vienna. 1963. p. 125.
10. R. Haas, W. Kley, K.H. Krebs, and R. Rubin. *In Inelastic scattering of neutrons in solids and liquids*. Vol. II. IAEA, Vienna. 1963. p. 145.
11. I. Pelah, R. Haas, W. Kley, K.H. Krebs, J. Peretti, and R. Rubin. *In Inelastic scattering of neutrons in solids and liquids*. Vol. II. IAEA, Vienna. 1963. p. 155.
12. B. Mozer, K. Otnes, and H. Palevsky. *In Lattice dynamics*. Edited by R.F. Wallis. Pergamon Press, Oxford. 1965. p. 63.
13. W. Gläser, F. Carvalho, and G. Ehret. *In Inelastic scattering of neutrons*. Vol. I. IAEA, Vienna. 1965. p. 99.
14. D.I. Page. *Proc. Phys. Soc.* **91**, 76 (1967).
15. M. Kamal, S.S. Malik, and D. Rorer. *Phys. Rev. B: Condens. Matter*, **18**, 1609 (1978).
16. E.C. Svensson, V.F. Sears, J.H. Root, C. Szornel, D.D. Klug, E. Whalley, and E.D. Hallman. *In Phonons 89*. Vol. I. Edited by S. Hunklinger, W. Ludwig, and G. Weiss. World Scientific, Singapore. 1990. p. 537.
17. D.D. Klug, E. Whalley, E.C. Svensson, V.F. Sears, J.H. Root, C. Szornel, and E.D. Hallman. *High Press. Res.* **4**, 528 (1990).
18. D.D. Klug, E. Whalley, E.C. Svensson, J.H. Root, and V.F. Sears. *Phys. Rev. B: Condens. Matter*, **44**, 841 (1991).
19. M.A. White, B.M. Powell, and V.F. Sears. *Mol. Cryst. Liq. Cryst.* **211**, 177 (1992).
20. V.F. Sears, B.M. Powell, J.S. Tse, C.I. Ratcliffe, and Y.P. Handa. *Physica B (Amsterdam)*, **180 & 181**, 658 (1992).
21. J.S. Tse, B.M. Powell, V.F. Sears, and Y.P. Handa. *Chem. Phys. Lett.* **215**, 383 (1993).
22. E.C. Svensson, W. Montfrooij, V.F. Sears, and D.D. Klug. *Physica B (Amsterdam)* **194-196**, 409 (1994).
23. D.D. Klug, E.C. Svensson, W. Montfrooij, and V.F. Sears. *AIP Conf. Proc.* **309**, 405 (1994).
24. C.B. Clark. *J. Grad. Res. Cent.* **29**, 10 (1961).
25. G.A. Alers. *Phys. Rev.* **119**, 1532 (1960).
26. V.F. Sears. *Adv. Phys.* **24**, 1 (1975).
27. A.A. Maradudin, E.W. Montroll, G.H. Weiss, and I.P. Ipatova. *Theory of lattice dynamics in the harmonic approximation*. 2nd ed. Academic Press Inc., New York. 1971.
28. L. Van Hove. *Phys. Rev.* **89**, 1189 (1953).
29. M.V. Linkoaho. *Philos. Mag.* **23**, 191 (1971).
30. R.D. Worley, M.W. Zemansky, and H.A. Boorse. *Phys. Rev.* **99**, 447 (1955).
31. W.S. Corak, B.B. Goodman, C.B. Satterthwaite, and A. Wexler. *Phys. Rev.* **102**, 656 (1956).
32. C.H. Cheng, K.P. Gupta, E.C. Van Reuth, and P.A. Beck. *Phys. Rev.* **126**, 2030 (1962).
33. G.A. Alers and J.R. Neighbours. *Rev. Mod. Phys.* **31**, 675 (1959).
34. G.L. Squires. *Introduction to the theory of thermal neutron scattering*. Cambridge University Press, Cambridge. 1978.
35. S.W. Lovesey. *Theory of neutron scattering from condensed matter*. Vol. I. Clarendon Press, Oxford. 1984.
36. A. Sjölander. *Ark. Fys.* **14**, 315 (1958).
37. V.F. Sears. *Phys. Rev. A: Gen. Phys.* **7**, 340 (1973).

## Appendix A: Multiphonon scattering

The expression (3.4) for the incoherent scattering function  $S(\mathbf{Q}, \nu)$  is originally due to Placzek and Van Hove [1] and is derived in most textbooks on thermal neutron scattering. However, the multiphonon terms are usually either ignored [34] or treated in an approximate fashion [35]. In fact, all the terms in the general multiphonon expansion of the incoherent scattering function of a harmonic crystal can be calculated exactly and expressed in the form of a recursion relation [36, 37], a form that is ideally suited to numerical calculations. In this appendix we review this expansion in the context of the present experiments on vanadium.

The general multiphonon expansion is of the form

$$S(\mathbf{Q}, \nu) = \sum_{n=0}^{\infty} S_n(\mathbf{Q}, \nu) \quad (\text{A1})$$

where  $n$  labels the contribution from  $n$ -phonon processes and

$$S_n(\mathbf{Q}, \nu) = S_n(\mathbf{Q})A_n(\nu) \quad (\text{A2})$$

In particular, for elastic scattering,

$$A_0(\nu) = \delta(\nu) \quad (\text{A3})$$

for one-phonon scattering,

$$A_1(\nu) = \frac{g(\nu)}{\gamma_0 \nu [1 - \exp(-\nu/\nu_0)]} \quad (\text{A4})$$

and for multiphonon scattering,

$$A_n(\nu) = \int_{-\infty}^{\infty} A_1(\nu - \nu')A_{n-1}(\nu') d\nu', \quad n \geq 2 \quad (\text{A5})$$

The quantity  $g(\nu)$  in (A4) is the phonon density of states, which is taken to be an even function of  $\nu$  and is normalized such that

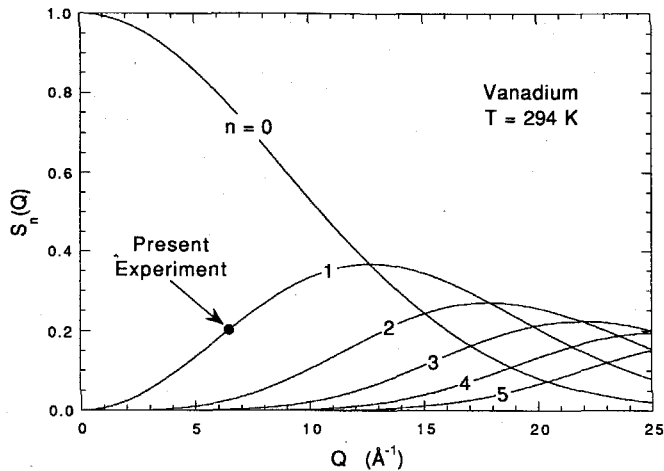
$$\int_0^{\infty} g(\nu) d\nu = 1 \quad (\text{A6})$$

Also,  $h\nu_0 = k_B T$ , in which  $T$  is the temperature, and

$$\gamma_0 = \int_0^{\infty} \coth\left(\frac{\nu}{2\nu_0}\right) \frac{g(\nu)}{\nu} d\nu \quad (\text{A7})$$

Strictly speaking, the quantity  $g(\nu)$  in (A4) is the velocity spectrum, i.e., the Fourier transform of the velocity autocorrelation function of an atom in the crystal, and this quantity depends on both the frequencies and polarization vectors of

**Fig. 8.** The integrated intensities  $S_n(Q)$  of the terms in the multiphonon expansion of the incoherent scattering function  $S(Q, \nu)$  for vanadium at 294 K calculated using the rms displacement  $u = 0.0789 \text{ \AA}$  determined in the present work. The dot indicates the one-phonon intensity at the momentum transfer  $Q = 6.5 \text{ \AA}^{-1}$  used in our experiments.



the phonons. It is only for a cubic Bravais lattice, such as the bcc structure of vanadium, that the polarization dependence vanishes and  $g(\nu)$  is simply equal to the phonon density of states.

The frequency-dependent factors  $A_n(\nu)$  have the property

$$\int_{-\infty}^{\infty} A_n(\nu) d\nu = 1, \quad n \geq 0. \quad (\text{A8})$$

so that  $S_n(Q)$  is the integrated intensity of the  $n$ th term:

$$S_n(Q) = \int_{-\infty}^{\infty} S_n(Q, \nu) d\nu \quad (\text{A9})$$

These quantities satisfy the sum rule

$$\sum_{n=0}^{\infty} S_n(Q) = \int_{-\infty}^{\infty} S(Q, \nu) d\nu = 1 \quad (\text{A10})$$

In general,

$$S_n(Q) = \frac{(2W)^n}{n!} e^{-2W} \quad (\text{A11})$$

in which  $e^{-2W}$  is the Debye-Waller factor, whose exponent is given by

$$2W = \nu_r \gamma_0 = (Qu)^2 \quad (\text{A12})$$

Here,  $h\nu_r$  is the recoil energy, which is defined by the relation

$$h\nu_r = \frac{(\hbar Q)^2}{2M} \quad (\text{A13})$$

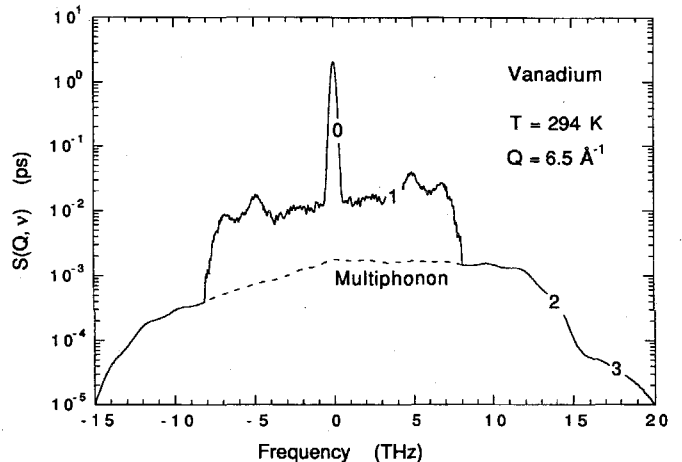
in which  $M$  is the atomic mass, and  $u$  is the root-mean-square (rms) displacement of an atom in the direction of  $Q$ .

Figure 8 shows the integrated intensities  $S_n(Q)$  as a function of  $Q$  for vanadium at 294 K calculated using the rms displacement  $u = 0.0789 \text{ \AA}$  determined in Sect. 4. The dot

**Table 4.** Values of the integrated intensities  $S_n(Q)$  of the terms in the multiphonon expansion of the incoherent scattering function  $S(Q, \nu)$  of vanadium at 294 K calculated at  $Q = 6.5 \text{ \AA}^{-1}$  using the rms displacement  $u = 0.0789 \text{ \AA}$  determined in the present work.

$n$	$S_n(Q)$
0	0.7686
1	0.2023
2	0.0266
3	0.0023
4	0.0002
Total	1.0000

**Fig. 9.** The reconstructed incoherent scattering function  $S(Q, \nu)$  for room-temperature vanadium calculated at  $Q = 6.5 \text{ \AA}^{-1}$  from the phonon density of states  $g(\nu)$  obtained in the present work. The numbers indicate the values of the multiphonon index  $n$  that dominate in various regions.



indicates the one-phonon intensity at the momentum transfer  $Q = 6.5 \text{ \AA}^{-1}$  used in our experiments. The numerical values of  $S_n(Q)$  at this value of  $Q$  are listed in Table 4. This value of  $Q$  was chosen so that we could measure the neutron scattering over the required energy range ( $-2$  to  $10$  THz) at reasonably high resolution. The integrated one-phonon intensity is a maximum when  $2W = 1$ , that is, when  $Q = u^{-1} = 12.7 \text{ \AA}^{-1}$ . However, if we had used this larger value of  $Q$  in our experiment, our resolution would have been considerably worse and the multiphonon scattering would have been very much larger than at  $6.5 \text{ \AA}^{-1}$ .

Once one has determined the phonon density of states  $g(\nu)$  from a neutron inelastic scattering experiment with  $0 \leq \nu \leq \nu_{\text{max}}$  and some specified values of  $Q$  and  $T$ , the entire incoherent scattering function  $S(Q, \nu)$  can be reconstructed for  $-\infty < \nu < \infty$  and any values of  $Q$  and  $T$ . Figure 9 shows such a reconstruction for the same values of  $Q$  and  $T$  that were used in our present experiment. The numbers indicate the values of the multiphonon index  $n$  that dominate in various regions. Thus, the (resolution-broadened) elastic scattering ( $n = 0$ ) dominates at  $\nu \approx 0$ , the one-phonon scattering ( $n = 1$ ) then dominates up to about  $\nu = 8.1$  THz,

the two-phonon scattering ( $n = 2$ ) up to about  $\nu = 16.2$  THz, and so on. The broken line in Fig. 9 indicates the total multiphonon contribution to  $S(\mathbf{Q}, \nu)$ . This is the estimate of the multiphonon scattering that was used earlier in Fig. 2.

### Appendix B: Multiple scattering

The multiple-scattering term  $C_{ms}$  in (3.2) is a sum of contributions from double, triple, and higher order scattering processes [26]. Each term in this expansion is given by an integral over a product of  $S(\mathbf{Q}, \nu)$ 's (one for each collision) and includes an additional factor that depends on the size, shape, and orientation of the sample relative to the incident beam. The integral is taken over all intermediate-neutron wave vectors. When the general multiphonon expansion (A1) for  $S(\mathbf{Q}, \nu)$  is substituted into these multiple-scattering integrals, one finds that the resulting expression for  $C_{ms}$  has a form similar to (3.4). In particular, the first term is proportional to  $\delta(\nu)$  and represents the contribution from multiple elastic scattering. The second term is proportional to  $A_1(\nu)$  (and, hence, to the phonon density of states  $g(\nu)$ ) and represents the contribution from processes in which the neutron is inelastically scattered by the emission or absorption of a single phonon in one of the collisions and is elastically scattered in all the other collisions. The remaining terms all

arise from collision sequences that involve multiple inelastic and (or) multiphonon processes. Unlike in (3.4), the coefficients of  $\delta(\nu)$  and  $A_1(\nu)$  in the multiple-scattering expansion of  $C_{ms}$  do not depend only on  $\mathbf{Q}$  but also on  $\nu$ . However, an inspection of the integrals involved indicates that these coefficients vary slowly and smoothly with  $\nu$ , much like the related quantity  $A$  in Fig. 3.

The above discussion suggests that little error is incurred by ignoring multiple scattering in the analysis of the neutron inelastic-scattering data to obtain the phonon density of states  $g(\nu)$ . The main effect of the multiple scattering is simply to alter the relative intensities of the elastic and one-phonon terms and to add an additional slowly varying background term. Thus, for example, if we ignore the effect of multiple scattering, and use (3.4) to obtain the Debye-Waller factor from the relative integrated intensity of the observed elastic peak, we find a value  $e^{-2W} = 0.822$  that is 7% larger than the value 0.769 that we calculated from the experimentally determined  $g(\nu)$  distribution. The latter value is expected to be the more accurate of the two. Similar discrepancies in the values of the Debye-Waller factors obtained by these two different methods were reported earlier by Page [14] and Kamal et al. [15].